INFECTIOUS DISEASE

Ketogenic diet activates protective γδ T cell responses against influenza virus infection

Emily L. Goldberg[1,2], Ryan D. Molony[2,3], Eriko Kudo[2], Sviatoslav Sidorov[1], Yong Kong[4], Vishwa Deep Dixit[1,2,5]*, Akiko Iwasaki[2,6,7]*

Influenza A virus (IAV) infection–associated morbidity and mortality are a key global health care concern, necessitating the identification of new therapies capable of reducing the severity of IAV infections. In this study, we show that the consumption of a low-carbohydrate, high-fat ketogenic diet (KD) protects mice from lethal IAV infection and disease. KD feeding resulted in an expansion of γδ T cells in the lung that improved barrier functions, thereby enhancing antiviral resistance. Expansion of these protective γδ T cells required metabolic adaptation to a ketogenic diet because neither feeding mice a high-fat, high-carbohydrate diet nor providing chemical ketone body substrate that bypasses hepatic ketogenesis protected against infection. Therefore, KD-mediated immune-metabolic integration represents a viable avenue toward preventing or alleviating influenza disease.

INTRODUCTION

Respiratory influenza A virus (IAV) infections are a major source of human morbidity and mortality, causing more than 20,000 deaths annually in the United States and incurring an economic burden in excess of $87 billion each year (*1*, *2*). Although an efficacious universal IAV vaccine is highly desirable and is under development (*3*, *4*), in its absence, novel therapeutic approaches are vital for the treatment of influenza diseases. Such therapeutic strategies can entail either improvements in viral resistance or enhancement of disease tolerance that alleviates lethal consequences of the viral infections (*5*, *6*). Disease tolerance strategies include providing energy substrates that aid in the metabolic adaptation required for host survival (*7*–*9*).

Inflammasome activation and neutrophil-mediated toxicity can promote tissue damage associated with IAV infections (*10*–*12*). In light of our recent findings that the ketone metabolite, β-hydroxybutyrate (BHB), inhibits Nod-like receptor family pyrin domain containing 3 (NLRP3) inflammasome–dependent interleukin-1β (IL-1β) secretion from neutrophils and macrophages (*13*, *14*), we hypothesized that ketogenic diet (KD) might also reduce IAV disease severity. To probe the effects of KD-induced BHB production on IAV disease in a physiologically relevant setting, we conducted all experiments in myxovirus protein 1 (Mx1)–congenic C57BL/6 mice (hereafter referred to as Mx1 mice). Mx1 is a dynamin-like guanosine triphosphatase that is a critical interferon (IFN)–inducible gene important for the control of primary IAV infections in mice (*15*, *16*). Most inbred mouse strains, including C57BL/6 mice, however, lack a functional copy of the Mx1 gene (*17*). Whereas wild-type C57BL/6 mice are extremely susceptible to IAV infection, succumbing to as few as 100 plaque-forming units (PFU) of A/PR8 IAV, Mx1 mice are highly resistant to infection with doses of more than 10^6 PFU (*10*, *18*, *19*). Therefore, in this study, we use Mx1 mice to probe the impact of KD on influenza infection and disease in the setting of intact innate immunity.

RESULTS

After intranasal challenge with IAV (10^8 PFU), Mx1 mice that had been fed KD for 7 days before infection were protected from body weight loss and had improved survival relative to mice on a normal chow diet (Fig. 1, A and B). In addition, KD-fed mice were able to better maintain blood O_2 saturation, suggesting improved gas exchange as compared with chow-fed mice (Fig. 1C). This observed protection was associated with improved antiviral resistance because viral titers were significantly lower in the lungs of KD-fed mice (Fig. 1D). To gain insight into the mechanisms underlying KD-enhanced antiviral immunity in the lungs of these mice, we performed transcriptome analysis of infected whole lung tissue samples (fig. S1 and table S1). KD did not result in enhanced IFNs or IFN-stimulated genes (ISGs). Instead, ingenuity pathway analysis (IPA) indicated enrichment in T cell activation pathways (fig. S1C). The results suggested that KD protects mice against IAV through nonconventional mechanisms with potential contribution from T cells early after IAV infection. Of the top 10 significantly regulated genes in KD-fed mice was a γδ T cell receptor (γδTCR) gene segment (*Tcrg-C1*), and by comparing our dataset with Immunological Genome Project γδ T cell datasets (*20*), we identified four additional genes in this list that are highly associated with γδ T cells (*Cxcr6*, *Blk*, *Cd163l1*, and *Ccr4*) (Fig. 1E). By flow cytometry, we observed significant increases in the frequencies and absolute numbers of γδ T cells in the lungs of KD-fed mice (Fig. 1, F to H), whereas no differences were found for other cell types tested (fig. S2A). Similar observations were also made in the bronchoalveolar lavage (BAL) (fig. S2, B to D). Intracellular cytokine staining identified these γδ T cells to be an IL-17–competent, but not IFN-γ–competent, subset (fig. S2, E and F). These IL-17–producing γδ T cells were recently shown to mediate neonatal influenza protection by inducing a type 2 innate lymphoid cell/regulatory T cell tissue repair response (*21*) and were essential for control of pulmonary bacterial infections (*22*–*24*). We did not

[1]Department of Comparative Medicine, Yale School of Medicine, New Haven, CT 06519, USA. [2]Department of Immunobiology, Yale School of Medicine, New Haven, CT 06519, USA. [3]Novartis Institutes for BioMedical Research, 250 Massachusetts Ave, Cambridge, MA 02139, USA. [4]Department of Molecular Biophysics and Biochemistry, W.M. Keck Foundation Biotechnology Resource Laboratory, Yale University School of Medicine, New Haven, CT 06520, USA. [5]Yale Center for Research on Aging, Yale School of Medicine, New Haven, CT 06519, USA. [6]Howard Hughes Medical Institute, Chevy Chase, MD 20815, USA. [7]Department of Molecular Cellular and Developmental Biology, Yale University, New Haven, CT, 06511, USA.
*Corresponding author. Email: vishwa.dixit@yale.edu (V.D.D.); akiko.iwasaki@yale.edu (A.I.).

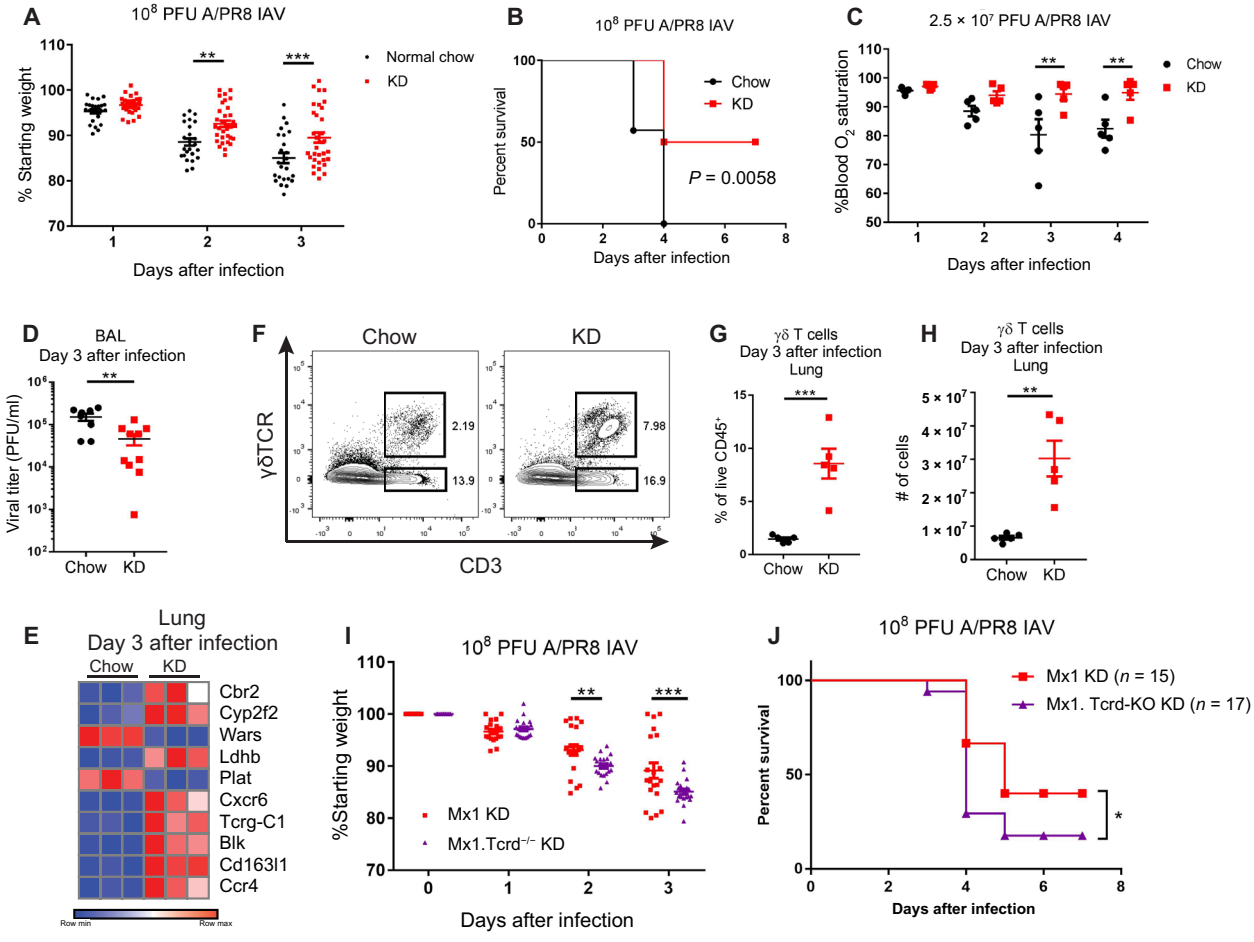

Fig. 1. γδ T cells are required for improved survival of KD-fed mice during IAV infection. (**A**) Body weight change (pooled from five independent experiments for a total of $n = 25$ chow and $n = 33$ KD mice analyzed) and (**B**) survival after infection with 10^8 PFU of A/PR8 IAV in chow ($n = 7$) versus KD ($n = 10$). Survival differences are representative of three independent experiments and were calculated by log-rank test. (**C**) Blood oxygen saturation kinetics after sublethal infection with 2.5×10^7 PFU of A/PR8 IAV. $n = 5$ mice per group. (**D**) BAL viral titers on day 3 after infection with 10^8 PFU of A/PR8 IAV. Pooled from two independent experiments (chow, $n = 8$; KD, $n = 10$). (**E**) Heat map of RNA-seq top 10 differentially expressed genes (day 3 after infection, based on adjusted $P < 0.05$) in IAV-infected whole lung tissue of KD-fed versus chow-fed mice. (**F**) Representative FACS plot of lung γδ T cells on day 3 after infection. (**G**) Percentage and (**H**) absolute number of γδ T cells in the lungs 3 days after IAV infection. $n = 5$ mice per group. (F to H) Data are representative of more than five independent experiments. (**I**) Body weight change after infection of Mx1 ($n = 21$) versus $Tcrd^{-/-}$ Mx1 mice fed KD ($n = 20$) with 10^8 PFU of IAV. Pooled from three independent experiments. (**J**) Survival after infection of Mx1 ($n = 15$) versus $Tcrd^{-/-}$ Mx1 mice fed KD ($n = 17$) with 10^8 PFU of IAV. Survival differences were calculated by the Gehan-Breslow-Wilcoxon test. (I) For all graphs, each symbol represents an individual mouse, and data are expressed as means ± SEM. Statistical differences were calculated by (A, C, and I) paired two-way ANOVA, and (D, G, and H) unpaired *t* test. $^*P < 0.05$, $^{**}P < 0.01$, $^{***}P < 0.001$.

detect differences in BAL IL-17 (fig. S2G), and we observed lower BAL IFN-γ levels (fig. S2H) in KD-fed mice compared with chow-fed mice on day 3 after infection. Although IPA indicated "T_H2 (T helper 2) activation" as a significantly regulated pathway in our dataset (fig. S1C), our transcriptome analysis did not reveal KD-induced enhancement of type 2 immunity genes identified by Guo *et al.* (*21*) (fig. S2I).

To assess the importance of γδ T cells in KD-mediated protection against influenza virus infection, we generated $Tcrd^{-/-}$ Mx1 mice and fed them either regular chow or KD before IAV infection. The protective effect of KD was diminished in $Tcrd^{-/-}$ Mx1 mice after lethal IAV infection (Fig. 1, I and J). These data indicate that γδ T cells are required for KD-mediated protection against influenza disease. $Tcrd^{-/-}$ mice on KD did not exhibit complete lethality, suggesting that multiple KD-induced physiological effects may synergize to improve IAV survival.

We considered the possibility that the enhanced body weight preservation in KD-fed mice might simply reflect the high caloric density of the diet (6.76 kcal/g, 90% of calories from fat, <1% of calories from carbohydrate) compared with standard chow diet (3.1 kcal/g, 18% of calories from fat, 58% of calories from carbohydrate). To test this, we compared the consequences of IAV infection in mice fed KD versus those fed standard high-fat diet (HFD; 5.21 kcal/g, 60% of calories from fat, 20% of calories from carbohydrate) beginning 1 week before infection. Unlike KD-fed mice, HFD-fed mice lost body weight upon IAV infection at levels comparable with mice on regular chow (Fig. 2A). Unexpectedly, HFD feeding also led to a significant increase in lung γδ T cells (Fig. 2B) that were also primed to produce IL-17 (Fig. 2C). Together, these data show that high-fat high-carbohydrate western diet–induced

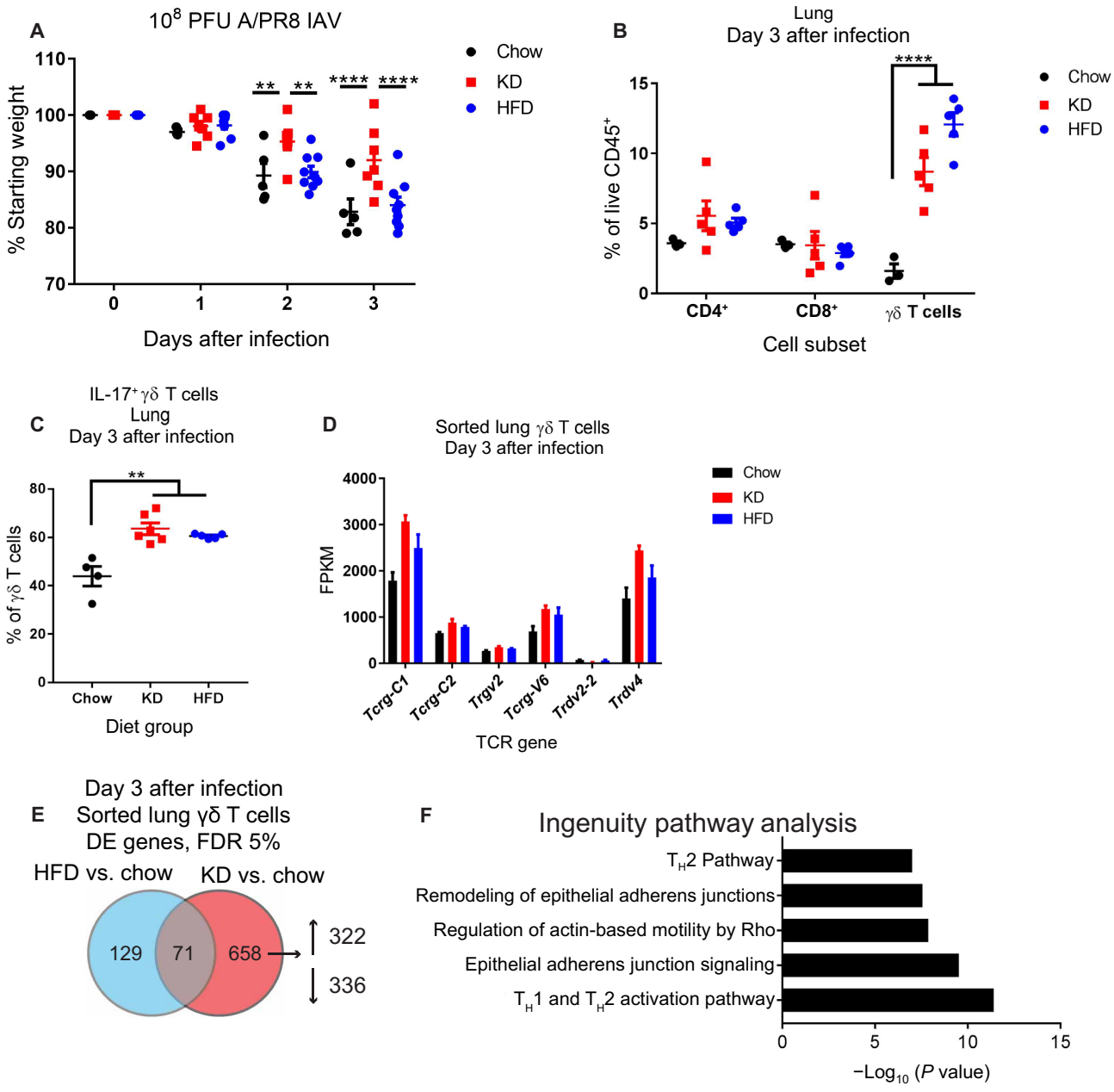

Fig. 2. High-fat content of KD is not sufficient to induce protective γδ T cells. (**A**) Body weight change of chow-fed ($n = 5$), KD-fed ($n = 7$), and HFD-fed ($n = 9$) mice after infection with 10^8 PFU of IAV. (**B**) Lung γδ T cell abundance 3 days after IAV infection in chow-fed ($n = 3$), KD-fed ($n = 5$), and HFD-fed ($n = 5$) mice. (**C**) Frequency of γδ T cells from the lungs of chow-fed ($n = 4$), KD-fed ($n = 6$), and HFD-fed ($n = 5$) mice that produce IL-17 after PMA + ionomycin stimulation ex vivo. (**D**) Bar graph of significantly regulated Tcrd and Tcrg gene segments. FPKM, fragments per kilobase per million mapped reads. (**E**) Venn diagram of numbers of differentially expressed (DE) genes (FDR, 5%) in chow, KD, and HFD sorted lung γδ T cells on day 3 after infection. (**F**) IPA of genes selectively induced by KD compared with chow. (A to C) Data are representative of three independent experiments. For all graphs, each symbol represents an individual mouse. Data are expressed as means ± SEM. Statistical differences were calculated by (A) paired two-way ANOVA, (B) two-way ANOVA with Tukey's correction for multiple comparisons, and (C) one-way ANOVA with Tukey's correction for multiple comparisons. $^{**}P < 0.01$, $^{****}P < 0.0001$.

expansion of γδ T cells is insufficient to confer protection, suggesting an important specificity for ketogenesis in protection against IAV infection.

To identify the potential link between diet-induced γδ T cells and protection against IAV infection, we probed for unique features of KD-induced γδ T cell phenotypes by RNA sequencing (RNA-seq) analysis of sorted γδ T cells from the lungs of mice fed chow versus HFD versus KD beginning 1 week before IAV infection (fig. S3 and tables S2 to S4). Certain γδTCR genes, including *Tcrg-C1* and *Trdv4*, were highly expressed among the sorted lung γδ T cells and were increased by KD (Fig. 2D), which suggested that rather than recruitment of an unexpected γδ T cell subset, protective functions of common γδ T cells were being enhanced. We found a relatively small list of genes (126 in total) that were differentially regulated [false discovery rate (FDR), 10%] by KD as compared with both chow and HFD (fig. S4A). All these genes except for one (*Tgtp1*) were regulated by KD

in the same direction compared with both chow and HFD (fig. S4, B and C). We noted KD-specific enrichment for multiple differentially regulated cytokines, ISGs, and effector molecules in this list, including the up-regulation of *Il-17a*, *Isg20*, *Ifit1bl1*, *Ifi204*, *Ctla4*, *Ccr1*, and *Cxcr4* and the down-regulation of *Il12rb2*, *P2rx7*, and *Ccr7* (fig. S4). IPA of the genes differentially regulated specifically by KD relative to normal chow (Fig. 2E) showed an enhancement of T_H2-type responses and enrichment for several pathways involved in epithelial cell adhesion functions (Fig. 2F and table S5). These data thus indicate that KD promotes the enrichment of a subset of lung γδ T cells with a unique genetic signature distinct from those induced by HFD.

We initially focused our analyses on day 3 after infection because most lethality occurred 4 days after infection (Fig. 1B). However, differences in body weight are apparent by day 2 after infection. We therefore decided to assess early changes induced by KD. KD-mediated increases in lung γδ T cells were evident before infection (fig. S5A) and remained elevated early after infection (fig. S5B). Like day 3 after infection, the expanded γδ T cells in the lungs 24 hours after infection were IL-17–competent and were mostly $CD44^+$ $CD27^-$ (fig. S5, C to E). Viral titers were similar in chow versus KD and HFD at this early time point after IAV infection (fig. S5F). In addition, despite previous studies showing neutrophil recruitment by γδ T cells (*25*, *26*), we found no differences in neutrophil or $Ly6C^+$ monocyte recruitment in the BAL during KD or HFD feeding (fig. S6).

Next, we examined the mechanisms by which γδ T cells accumulate in the lungs in response to KD feeding. KD increased bromo deoxyuridine (BrdU) incorporation in γδ T cells (fig. S7A), suggesting increased proliferation of these cells. Blockade of Giα signaling via treatment with pertussis toxin (PTx) impeded γδ T cell expansion in KD-fed mice (fig. S7B). Together, these results suggest that both proliferation and chemokine-mediated recruitment drive the γδ T cell expansion in response to KD during IAV infection.

Given that BHB serves as the primary energy substrate during glucose deprivation and KD feeding (*27*), we next tested whether BHB itself was responsible for the γδ T cell increase in the lungs after IAV infection. To test this possibility, we fed mice 1,3-butanediol (BD), which increases circulating BHB levels without the requirement for mitochondrial fatty acid oxidation, a necessary metabolic switch induced by KD. Although BD efficiently elevated blood BHB to levels comparable with KD-fed mice, it failed to induce γδ T cell expansion or to protect Mx1 mice from IAV-induced weight loss (Fig. 3, A and B), indicating that BHB is not sufficient to mediate this phenotype. These data indicate that metabolic adaptation favoring enhanced fatty acid oxidation during KD feeding (*28*), rather than a simple increase in BHB levels, is required for the expansion of protective γδ T cells in the lung and the maintenance of body weight during IAV infection. In further support of this hypothesis, we examined proteins essential for oxidative mitochondrial

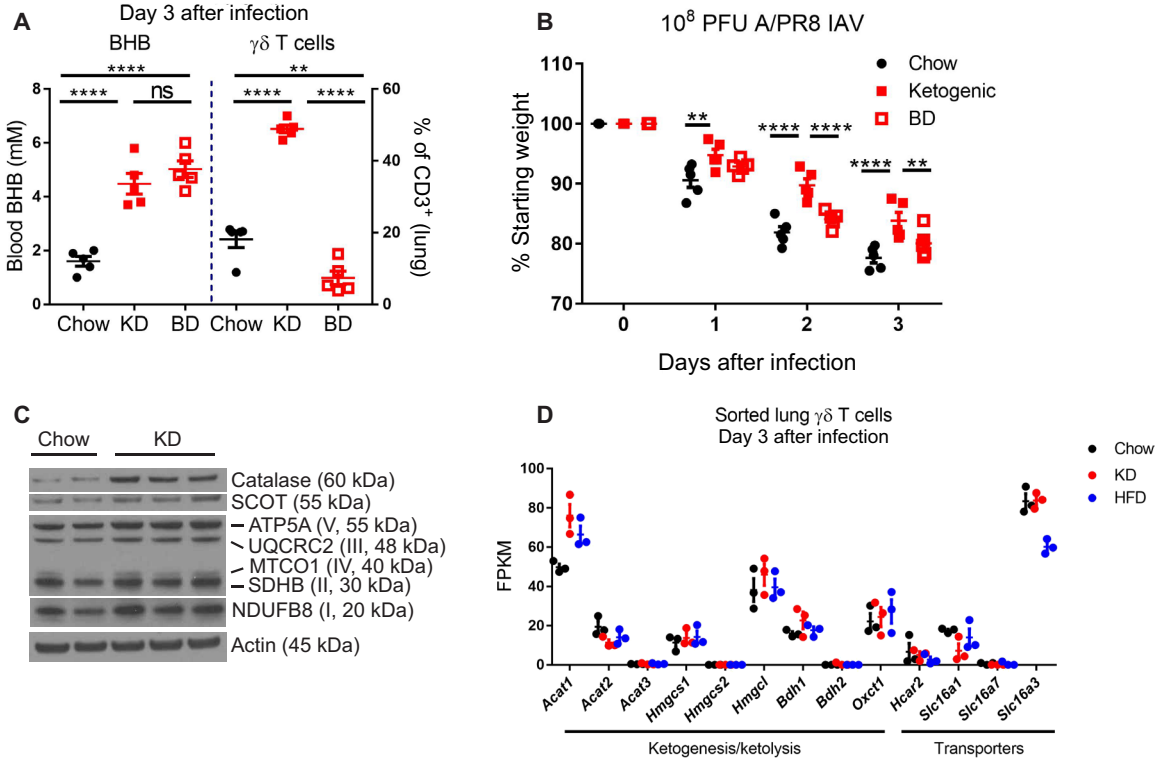

Fig. 3. Protective γδ T cell expansion requires metabolic adaptation to KD. (**A**) Blood BHB and lung γδ T cells on day 3 after IAV infection in mice fed chow ($n = 5$) versus KD ($n = 5$) versus BD ($n = 5$) beginning 1 week before infection. Statistical differences were calculated by one-way ANOVA with Tukey's correction for multiple comparisons. ns, not significant. (**B**) Body weights of IAV-infected mice fed chow ($n = 5$), KD ($n = 5$), or BD ($n = 5$). Statistical differences were calculated by paired two-way ANOVA with Tukey's correction for multiple comparisons. (A and B) Data are representative of at least two independent repeats. (**C**) Western blot of mitochondrial oxidative metabolism proteins in whole lung tissue 3 days after IAV infection in chow- and KD-fed mice. Each lane represents an individual mouse. (**D**) RNA-seq expression data of ketone metabolism genes from sorted γδ T cells 3 days after infection. For all graphs, each symbol represents an individual mouse. Data are expressed as means ± SEM. $^{**}P < 0.01$, $^{****}P < 0.0001$.

metabolism in the lung and observed that KD-fed mice displayed higher expression of catalase, a key enzyme that protects against reactive oxygen species damage, and 3-oxoacid coenzyme A transferase 1 (*Oxct1* or SCOT), a rate-limiting enzyme in mitochondrial ketolysis (Fig. 3C). In addition, as compared with chow-fed mice, those fed KD also showed elevated expression of mitochondrial electron transport chain complexes in the lungs (Fig. 3C). Neither KD nor HFD altered ketone metabolism genes specifically in γδ T cells (Fig. 3D), and although KD induced gene signatures associated with increased oxidative phosphorylation metabolic programming, ketone metabolism pathways were not significantly altered by KD in sorted γδ T cells (fig. S3 and table S4). Together, these data demonstrate that KD-dependent increased oxidative metabolism and improved redox balance in the lung are linked with γδ T cell expansion and enhanced survival in response to an otherwise lethal IAV infection.

To identify the molecular basis for γδ T cell–mediated protection against IAV lethality, we performed RNA-seq on IAV-infected lungs from KD-fed *Tcrd*$^{-/-}$ Mx1 mice (fig. S8 and table S6). We identified a variety of genes significantly regulated by KD and manually clustered them based on γδ T cell dependence (fig. S9). We analyzed the intersection of genes significantly regulated by KD that were also γδ T cell dependent and identified 11 genes that met these criteria (Fig. 4A). This gene list indicated that KD, in a γδ T cell–dependent manner, increased protective airway secretory cells (*Scgb1a1* and *Scgb3a2*), scavenger receptors *Cd163l1* (possibly due to its expression on γδ T cells), and *Marco* (*Scgb3a2* binding partner). These genes also suggested that, in a γδ T cell–dependent manner, KD improved pulmonary metabolism of endogenous carbonyl compounds including ketones derived from lipid peroxidation (*Cbr2*), metabolism of toxic compounds (*Cyp2f2* and *Cyp4f15*), and increased tight junctions (*Cldn10*) (Fig. 4A). This pattern of gene enrichment suggested enhanced secretory cell function in the lung in response to KD. Periodic acid–Schiff (PAS) staining used to identify mucus-producing cells confirmed an increase in the numbers of mucus-producing cells in the airways of KD-fed mice that were dependent on γδ T cells (Fig. 4, B to H). Accordingly, the expression of *Scgb1a1*, a specific marker of club cells and a founding member of the secretoglobin family, correlated with decreasing viral titers in the lung (Fig. 4H).

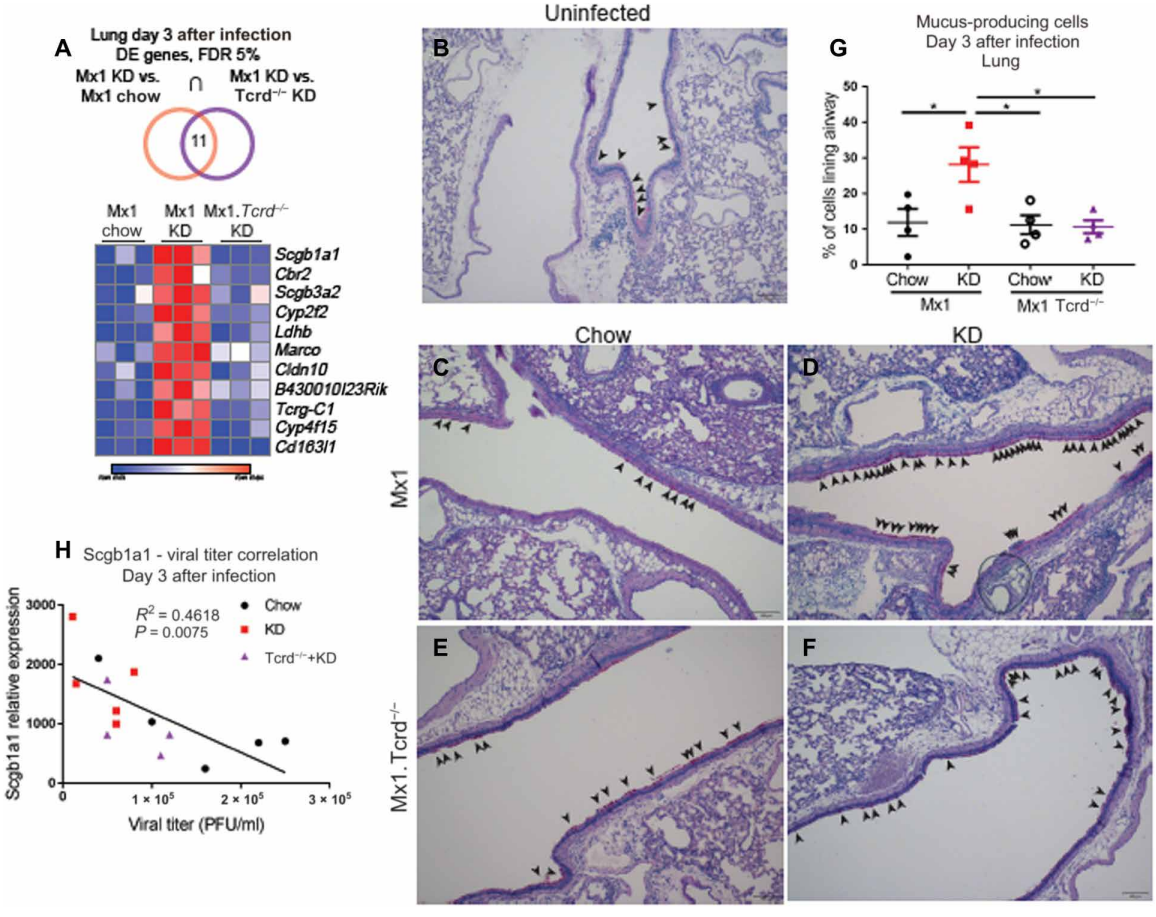

Fig. 4. KD-induced protective γδ T cells enhance lung barrier function. (**A**) Heat map of significantly regulated genes (based on adjusted $P < 0.05$) in both comparisons of Mx1 chow versus Mx1 KD, and Mx1 KD versus Mx1 Tcrd$^{-/-}$ KD. Genes are ranked from highest to lowest expression. (**B** to **F**) Representative images of lung airway PAS staining. Arrowheads indicate PAS-positive cells. Scale bars, 100 μm. (**G**) Quantification of PAS staining images. Statistical differences were calculated by one-way ANOVA with Tukey's correction for multiple comparisons. Data are represented as means ± SEM and $n = 4$ mice per group. (**H**) Correlation analysis of lung Scgb1a1 expression with BAL viral titers collected on day 3 after IAV infection. Statistics were calculated by linear regression pooled from chow ($n = 5$), KD ($n = 5$), and Mx1 *Tcrd*$^{-/-}$ KD ($n = 4$). For all graphs, each symbol represents an individual mouse. *$P < 0.05$.

DISCUSSION

Our study found that KD feeding confers protection against influenza virus infection in Mx1 mice. KD increased the number of γδ T cells in the respiratory tract, and these γδ T cells were required to achieve the full protective effect of KD. The contributions of γδ T cells to lung homeostasis and IAV immunity remain incompletely explored. γδ T cells have previously been reported to increase late after IAV infection in mice (*29*). Human γδ T cells can expand in a TCR-independent manner in response to IAV, and the human Vγ9Vδ2 T cell subset has been shown to efficiently induce the cytolytic killing of IAV-infected A549 airway cells (*30*, *31*). The precise mechanism by which KD-induced γδ T cells enhance lung barrier integrity will require further study.

How might γδ T cells protect the host against influenza virus challenge in response to KD? Our results may be explained by efficient killing of IAV-infected airway epithelial cells by the γδ T cells, which expand specifically in response to KD in mice, resulting in lower viral titers and overall better preservation of airway tissue integrity. However, the transcriptome data did not reveal any canonical cytotoxicity genes uniquely induced by KD (fig. S4). Alternatively, the γδ T cells induced by KD may enhance the barrier and innate defense functions of airway epithelial cells at baseline, thus allowing them to better respond upon IAV challenge, leading to observed lower viral titers. Consistent with this latter model, KD-fed mice increased mucus-producing cells in the airway in a γδ T cell–dependent manner. In addition, RNA-seq analysis of infected lung tissue revealed unique epithelial gene patterns that were associated with lower viral titer and improved survival that were lost in KD-fed *Tcrd*$^{-/-}$ mice.

Other studies have shown that epithelial γδ T cells improve lung integrity both in the context of bacterial infection and ozone exposure (*32*), whereas *Tcrd*$^{-/-}$ mice are more susceptible to mucosal injury in a dextran sulfate sodium–colitis model (*33*). Collectively, these studies highlight a key role for γδ T cells in maintaining barrier integrity beyond their cytolytic potential. This possibility is further supported by a recent report that adipose tissue γδ T cells have critical protective functions during cold stress (*34*). Our results showed the capacity of KD, but not HFD, in conferring protection against influenza virus infection. Further, KD-mediated protection relied in large part on the presence of γδ T cells. We propose that γδ T cells may serve as a modulator of epithelial functionality in response to diet and nutrient availability, by inducing changes in the epithelial cell differentiation and function for adaptation to the changing environment. Harnessing the beneficial effects of KD through γδ T cells may therefore offer a potential previously unrecognized avenue for influenza disease prevention and treatment.

MATERIALS AND METHODS

Study design

The objective of this study was to determine how KD feeding affects host defense against lethal IAV infection. Mice were randomized to indicated diet groups for 1 week before infection and were subsequently monitored for clinical signs of disease and euthanized to assess the immune response against IAV. The different diets used are visibly different, so investigator blinding during experiments was impossible, but genotypes and diet groups were deidentified during analysis to blind investigators during this phase of the experiments. Group sizes are indicated in respective figure legends. None of the data shown contained any statistical outliers. All experiments were repeated independently at least three times.

Mice

All mice were C57BL/6 carrying functional alleles of Mx1 as previously reported (*35*). *Tcrd*$^{-/-}$ mice (purchased from the Jackson laboratory) (*36*) were originally on the B6 background and then crossed with Mx1 mice in the Iwasaki lab to generate homozygous knockout mice for each genotype. Mice were housed under specific pathogen–free conditions under normal 12-hour light/dark cycles in the Yale animal facility. All procedures were approved by the Yale Institutional Animal Care and Use Committee.

Diets

All diets were provided ad libitum throughout experiments. Mice were maintained on standard vivarium chow (Envigo 2018S) until switched to respective experimental diets exactly 1 week before infection. KD (D12369B) and HFD (60%; D12492) were purchased from Research Diets. BD diet was prepared by mixing standard chow (198 g; Purina 5002) + BD (80 ml; Sigma-Aldrich) + H_2O (120 ml) + saccharine (2 g; Sigma-Aldrich) and replaced daily.

Infection and treatments

Mice were anesthetized by intraperitoneal injection of ketamine and xylazine and were then infected intranasally with 10^8 PFU of A/PR/8/34 (H1N1) influenza virus in a total volume of 50 μl. Mice were monitored daily for body weight changes. BHB was measured in whole blood by handheld Precision Xtra test strips. Mice were treated with 500 ng of PTx in 50 μl of phosphate-buffered saline (PBS) by daily intraperitoneal injection immediately after infection. BrdU was provided in drinking water at 0.8 mg/ml + 5 mM saccharin beginning 1 day before infection and changed every other day. Blood O_2 saturation was measured by pulse oximetry (MouseOx Plus, STARR Life Sciences) in mice infected with a sublethal IAV dose (2.5×10^7 PFU) so that all mice would survive infection.

Measurement of viral titers

BAL was collected by washing the trachea and lungs three times with 1 ml PBS + 0.1% bovine serum albumin (BSA). Tenfold serial dilutions of BAL were made in 100-μl aliquots of PBS + 0.1% BSA and used to inoculate Madin-Darby canine kidney cells in 12-well plates. After 1 hour of incubation, each well was overlaid with 1 ml of agar medium for 48 hours. Cell monolayers were then stained with 0.1% crystal violet in 20% ethanol, and plaques were enumerated.

Western blot

Whole lung tissue was snap frozen in liquid nitrogen and homogenized in radioimmunoprecipitation assay buffer containing protease inhibitors. Protein concentration was measured by DC Protein Assay (Bio-Rad), and equal amounts of protein were run on an SDS-polyacrylamide gel electrophoresis and transferred to nitrocellulose membrane using standard techniques. Blots were probed with primary antibodies against catalase (Sigma-Aldrich), SCOT (Proteintech), electron transport chain complexes (samples were prepared according to manufacturer's recommendation; Abcam), and actin (Cell Signaling Technology). Incubation in secondary antibodies of the appropriate species (ThermoFisher Scientific) was followed by chemiluminescent visualization (ThermoFisher Scientific, Bio-Rad).

Flow cytometry

Lungs were digested for 1 hour in RPMI + 10% fetal calf serum + 1 mM $CaCl_2$ + 1 mM $MgCl_2$ + 5 mM Hepes + 2.5% collagenase D. Tissue

was minced through a 70-μm strainer to obtain a single-cell suspension. Cells were stained with live/dead viability dye (Invitrogen) followed by surface staining for B220, CD11b, NK1.1, CD3, CD4, CD8, and γδTCR. BrdU incorporation was detected by BrdU staining using the BD BrdU flow kit staining protocol. For intracellular cytokine staining, lung cells were stimulated at 37°C with phorbol 12-myristate 13-acetate (PMA; 10 ng/ml; Sigma) + ionomycin (1 μM; Sigma) for 4 hours, and protein transport inhibitor (eBioscience) was added for the last 3 hours of stimulation. Intracellular IL-17 and IFNγ staining were detected using the BD fix/perm staining kit. Cell counts were obtained by normalizing to CountBright Absolute Counting Beads (ThermoFisher Scientific).

RNA sequencing

Whole transcriptome analysis was performed in whole lung tissue and also in γδ T cells isolated by fluorescence-activated cell sorting (FACS) from digested lung tissue. The quality of raw reads was assessed with FastQC (*37*). Raw reads were mapped to the GENCODE vM9 mouse reference genome (*38*) using STAR aligner (*39*) with the following options: --outFilterMultimapNmax 15 --outFilterMismatchNmax 6 --outSAMstrandField All --outSAMtype BAM SortedByCoordinate --quantMode TranscriptomeSAM. The quality control of mapped reads was performed using in-house scripts that use Picard tools (*40*). The list of ribosomal RNA (rRNA) genomic intervals that we used for this quality control was prepared on the basis of UCSC mm10 rRNA annotation file (*41*) and GENCODE primary assembly annotation for vM9 (*38*). rRNA intervals from these two annotations were combined and merged to obtain the final list of rRNA intervals. These intervals were used for the calculation of the percentage of reads mapped to rRNA genomic loci. Principal components analysis (PCA) was performed in R. On the basis of the PCA, we excluded one sample from the whole lung dataset, but none from the sorted γδ T cell dataset, from further analysis as an outlier. Gene differential expression was calculated using DESeq2 (*42*). Pathway analysis was performed using IPA (QIAGEN) (*43*) and fgsea (fast gene set enrichment analysis) R package (*44*) with the minimum of 15 genes and maximum of 500 genes in a pathway and with 1 million permutations. For the pathway analysis, we used the canonical pathways from the MSigDB C2 pathway set v6.1 (*45*, *46*).

Quantitative polymerase chain reaction

Select genes of interest from RNA-seq dataset in whole lung tissue were independently verified by quantitative reverse transcription polymerase chain reaction (RT-PCR). Lungs were snap frozen in liquid nitrogen and homogenized directly in RLT buffer for RNA extraction (QIAGEN). RNA was quantified, and complementary DNA (cDNA) was transcribed using iScript cDNA synthesis kit (Bio-Rad). Gene expression was measured by RT-PCR by $\Delta\Delta C_t$ method and expressed relative to hypoxanthine-guanine phosphoribosyltransferase (Hprt) or glyceraldehyde-3-phosphate dehydrogenase (Gapdh). Relative expression was used for correlation analyses.

Immunohistochemistry

PAS staining was performed on formalin-fixed paraffin-embedded lung tissue sections. Sections were deparrafinized in xylenes and rehydrated in ethanol (EtOH) using standard procedures. PAS staining was performed exactly according to the manufacturer's protocol using the PAS staining kit (Sigma-Aldrich). Slides were then dehydrated in EtOH and cleared in xylenes for mounting. Images were acquired on a KEYENCE BZ-X700 microscope.

Statistical analysis

All analyses, except for RNA-seq, were performed using GraphPad Prism 7 software. To compare changes over time between different groups, paired two-way analysis of variance (ANOVA) with Tukey's correction for multiple comparisons was used to calculate statistical differences. Survival was based on 20% body weight loss, and statistical significance was calculated by log-rank test. Statistical differences comparing three groups were calculated by one-way ANOVA with Tukey's correction for multiple comparisons. Unpaired two-tailed *t* tests were used to calculate statistical differences between two groups. Correlation analyses were performed using linear regression. For all tests, $P \leq 0.05$ was considered statistically significant. $^{*}P < 0.05$, $^{**}P < 0.01$, $^{***}P < 0.001$, and $^{****}P < 0.0001$.

SUPPLEMENTARY MATERIALS

immunology.sciencemag.org/cgi/content/full/4/41/eaav2026/DC1

Fig. S1. Bioinformatics workflow for whole lung RNA-seq analysis.
Fig. S2. Quantification and phenotype of lung γδ T cells 3 days after IAV infection.
Fig. S3. RNA-seq bioinformatics of sorted lung γδ T cells 3 days after IAV infection.
Fig. S4. Transcriptomic signature of KD-specific genes in lung γδ T cells 3 days after IAV infection.
Fig. S5. γδ T cells expansion precedes IAV infection.
Fig. S6. Inflammatory myeloid cell infiltration is not affected by KD or HFD.
Fig. S7. Proliferation and recruitment drive KD-mediated γδ T cell expansion.
Fig. S8. Bioinformatics workflow for whole lung RNA-seq analysis in Mx1 Tcrd$^{-/-}$ mice.
Fig. S9. γδ T cell–dependent regulation of KD-induced transcriptome changes.
Table S1. Significantly regulated pathways in whole lungs of chow versus KD mice 3 days after IAV infection.
Table S2. Gene set enrichment analysis of sorted lung γδ T cells from HFD-fed versus KD-fed mice.
Table S3. Gene set enrichment analysis of sorted lung γδ T cells from HFD-fed versus chow-fed mice.
Table S4. Gene set enrichment analysis of sorted lung γδ T cells from KD-fed versus chow-fed mice.
Table S5. KD-specific gene signature of lung γδ T cells.
Table S6. Significantly regulated pathways in whole lungs of Mx1 KD versus Mx1 Tcrd$^{-/-}$ KD mice 3 days after IAV infection.

View/request a protocol for this paper from *Bio-protocol*.

REFERENCES AND NOTES

1. W. W. Thompson, E. Weintraub, P. Dhankhar, P.-Y. Cheng, L. Brammer, M. I. Meltzer, J. S. Bresee, D. K. Shay, Estimates of US influenza-associated deaths made using four different methods. *Influenza Other Respi. Viruses* **3**, 37–49 (2009).
2. N.-A. M. Molinari, I. R. Ortega-Sanchez, M. L. Messonnier, W. W. Thompson, P. M. Wortley, E. Weintraub, C. B. Bridges, The annual impact of seasonal influenza in the US: measuring disease burden and costs. *Vaccine* **25**, 5086–5096 (2007).
3. J. R. Ortiz, J. Hickling, R. Jones, A. Donabedian, O. G. Engelhardt, J. M. Katz, S. A. Madhi, K. M. Neuzil, G. F. Rimmelzwaan, J. Southern, D. J. Spiro, J. Hombach, Report on eighth WHO meeting on development of influenza vaccines that induce broadly protective and long-lasting immune responses: Chicago, USA, 23-24 August 2016. *Vaccine* **36**, 932–938 (2018).
4. C. I. Paules, H. D. Marston, R. W. Eisinger, D. Baltimore, A. S. Fauci, The pathway to a universal influenza vaccine. *Immunity* **47**, 599–603 (2017).
5. A. Iwasaki, P. S. Pillai, Innate immunity to influenza virus infection. *Nat. Rev. Immunol.* **14**, 315–328 (2014).
6. R. Medzhitov, D. S. Schneider, M. P. Soares, Disease tolerance as a defense strategy. *Science* **335**, 936–941 (2012).
7. G. F. Cahill Jr., R. L. Veech, Ketoacids? Good medicine? *Trans. Am. Clin. Climatol. Assoc.* **114**, 149–161; discussion 162–3 (2003).
8. A. Wang, S. C. Huen, H. H. Luan, S. Yu, C. Zhang, J.-D. Gallezot, C. J. Booth, R. Medzhitov, Opposing effects of fasting metabolism on tissue tolerance in bacterial and viral inflammation. *Cell* **166**, 1512–1525.e12 (2016).

9. J. C. Newman, E. Verdin, Ketone bodies as signaling metabolites. *Trends Endocrinol. Metab.* **25**, 42–52 (2014).
10. P. S. Pillai, R. D. Molony, K. Martinod, H. Dong, I. K. Pang, M. C. Tal, A. G. Solis, P. Bielecki, S. Mohanty, M. Trentalange, R. J. Homer, R. A. Flavell, D. D. Wagner, R. R. Montgomery, A. C. Shaw, P. Staeheli, A. Iwasaki, Mx1 reveals innate pathways to antiviral resistance and lethal influenza disease. *Science* **352**, 463–466 (2016).
11. M. Brandes, F. Klauschen, S. Kuchen, R. N. Germain, A systems analysis identifies a feedforward inflammatory circuit leading to lethal influenza infection. *Cell* **154**, 197–212 (2013).
12. T. Mauad, L. A. Hajjar, G. D. Callegari, L. F. F. da Silva, D. Schout, F. R. B. G. Galas, V. A. F. Alves, D. M. A. C. Malheiros, J. O. C. Auler Jr., A. F. Ferreira, M. R. L. Borsato, S. M. Bezerra, P. S. Gutierrez, E. T. E. G. Caldini, C. A. Pasqualucci, M. Dolhnikoff, P. H. N. Saldiva, Lung pathology in fatal novel human influenza A (H1N1) infection. *Am. J. Respir. Crit. Care Med.* **181**, 72–79 (2010).
13. E. L. Goldberg, J. L. Asher, R. D. Molony, A. C. Shaw, C. J. Zeiss, C. Wang, L. A. Morozova-Roche, R. I. Herzog, A. Iwasaki, V. D. Dixit, β-Hydroxybutyrate deactivates neutrophil NLRP3 inflammasome to relieve gout flares. *Cell Rep.* **18**, 2077–2087 (2017).
14. Y.-H. Youm, K. Y. Nguyen, R. W. Grant, E. L. Goldberg, M. Bodogai, D. Kim, D. D'Agostino, N. Planavsky, C. Lupfer, T. D. Kanneganti, S. Kang, T. L. Horvath, T. M. Fahmy, P. A. Crawford, A. Biragyn, E. Alnemri, V. D. Dixit, The ketone metabolite β-hydroxybutyrate blocks NLRP3 inflammasome-mediated inflammatory disease. *Nat. Med.* **21**, 263–269 (2015).
15. J. Verhelst, E. Parthoens, B. Schepens, W. Fiers, X. Saelens, Interferon-inducible protein Mx1 inhibits influenza virus by interfering with functional viral ribonucleoprotein complex assembly. *J. Virol.* **86**, 13445–13455 (2012).
16. O. Haller, P. Staeheli, M. Schwemmle, G. Kochs, Mx GTPases: Dynamin-like antiviral machines of innate immunity. *Trends Microbiol.* **23**, 154–163 (2015).
17. P. Staeheli, R. Grob, E. Meier, J. G. Sutcliffe, O. Haller, Influenza virus-susceptible mice carry Mx genes with a large deletion or a nonsense mutation. *Mol. Cell. Biol.* **8**, 4518–4523 (1988).
18. M. M. Kaminski, A. Ohnemus, M. Cornitescu, P. Staeheli, Plasmacytoid dendritic cells and Toll-like receptor 7-dependent signalling promote efficient protection of mice against highly virulent influenza A virus. *J. Gen. Virol.* **93**, 555–559 (2012).
19. K. Moritoh, H. Yamauchi, A. Asano, K. Yoshii, H. Kariwa, I. Takashima, N. Isoda, Y. Sakoda, H. Kida, N. Sasaki, T. Agui, Generation of congenic mouse strains by introducing the virus-resistant genes, Mx1 and Oas1b, of feral mouse-derived inbred strain MSM/Ms into the common strain C57BL/6J. *Jpn. J. Vet. Res.* **57**, 89–99 (2009).
20. T. S. P. Heng, M. W. Painter; Immunological Genome Project Consortium, K. Elpek, V. Lukacs-Kornek, N. Mauermann, S. J. Turley, D. Koller, F. S. Kim, A. J. Wagers, N. Asinovski, S. Davis, M. Fassett, M. Feuerer, D. H. D. Gray, S. Haxhinasto, J. A. Hill, G. Hyatt, C. Laplace, K. Leatherbee, D. Mathis, C. Benoist, R. Jianu, D. H. Laidlaw, J. A. Best, J. Knell, A. W. Goldrath, J. Jarjoura, J. C. Sun, Y. Zhu, L. L. Lanier, A. Ergun, Z. Li, J. J. Collins, S. A. Shinton, R. R. Hardy, R. Friedline, K. Sylvia, J. Kang, The Immunological Genome Project: Networks of gene expression in immune cells. *Nat. Immunol.* **9**, 1091–1094 (2008).
21. X.-z. J. Guo, P. Dash, J. C. Crawford, E. K. Allen, A. E. Zamora, D. F. Boyd, S. Duan, R. Bajracharya, W. A. Awad, N. Apiwattanakul, P. Vogel, T.-D. Kanneganti, P. G. Thomas, Lung γδ T cells mediate protective responses during neonatal influenza infection that are associated with type 2 immunity. *Immunity* **49**, 531–544.e6 (2018).
22. A. C. Kirby, D. J. Newton, S. R. Carding, P. M. Kaye, Evidence for the involvement of lung-specific γδ T cell subsets in local responses to *Streptococcus pneumoniae* infection. *Eur. J. Immunol.* **37**, 3404–3413 (2007).
23. Y. Okamoto Yoshida, M. Umemura, A. Yahagi, R. L. O'Brien, K. Ikuta, K. Kishihara, H. Hara, S. Nakae, Y. Iwakura, G. Matsuzaki, Essential role of IL-17A in the formation of a mycobacterial infection-induced granuloma in the lung. *J. Immunol.* **184**, 4414–4422 (2010).
24. P. L. Simonian, C. L. Roark, F. Wehrmann, A. M. Lanham, W. K. Born, R. L. O'Brien, A. P. Fontenot, IL-17A-expressing T cells are essential for bacterial clearance in a murine model of hypersensitivity pneumonitis. *J. Immunol.* **182**, 6540–6549 (2009).
25. B. Yan, F. Chen, L. Xu, J. Xing, X. Wang, HMGB1-TLR4-IL23-IL17A axis promotes paraquat-induced acute lung injury by mediating neutrophil infiltration in mice. *Sci. Rep.* **7**, 597 (2017).
26. F. Ramirez-Valle, E. E. Gray, J. G. Cyster, Inflammation induces dermal $V\gamma4^+\gamma\delta$T17 memory-like cells that travel to distant skin and accelerate secondary IL-17–driven responses. *Proc. Natl. Acad. Sci. U.S.A.* **112**, 8046–8051 (2015).
27. P. Puchalska, P. A. Crawford, Multi-dimensional roles of ketone bodies in fuel metabolism, signaling, and therapeutics. *Cell Metab.* **25**, 262–284 (2017).
28. A. R. Kennedy, P. Pissios, H. Otu, R. Roberson, B. Xue, K. Asakura, N. Furukawa, F. E. Marino, F. F. Liu, B. B. Kahn, T. A. Libermann, E. Maratos-Flier, A high-fat, ketogenic diet induces a unique metabolic state in mice. *Am. J. Physiol. Endocrinol. Metab.* **292**, E1724–E1739 (2007).
29. S. R. Carding, W. Allan, S. Kyes, A. Hayday, K. Bottomly, P. C. Doherty, Late dominance of the inflammatory process in murine influenza by gamma/delta + T cells. *J. Exp. Med.* **172**, 1225–1231 (1990).
30. Y. Lu, Z. Li, C. Ma, H. Wang, J. Zheng, L. Cui, W. He, The interaction of influenza H5N1 viral hemagglutinin with sialic acid receptors leads to the activation of human γδ T cells. *Cell. Mol. Immunol.* **10**, 463–470 (2013).
31. H. Li, Z. Xiang, T. Feng, J. Li, Y. Liu, Y. Fan, Q. Lu, Z. Yin, M. Yu, C. Shen, W. Tu, Human Vγ9Vδ2-T cells efficiently kill influenza virus-infected lung alveolar epithelial cells. *Cell. Mol. Immunol.* **10**, 159–164 (2013).
32. D. P. King, D. M. Hyde, K. A. Jackson, D. M. Novosad, T. N. Ellis, L. Putney, M. Y. Stovall, L. S. Van Winkle, B. L. Beaman, D. A. Ferrick, Cutting edge: Protective response to pulmonary injury requires γδ T lymphocytes. *J. Immunol.* **162**, 5033–5036 (1999).
33. Y. Chen, K. Chou, E. Fuchs, W. L. Havran, R. Boismenu, Protection of the intestinal mucosa by intraepithelial γδ T cells. *Proc. Natl. Acad. Sci. U.S.A.* **99**, 14338–14343 (2002).
34. A. C. Kohlgruber, S. T. Gal-Oz, N. M. LaMarche, M. Shimazaki, D. Duquette, H.-F. Koay, H. N. Nguyen, A. I. Mina, T. Paras, A. Tavakkoli, U. von Andrian, A. P. Uldrich, D. I. Godfrey, A. S. Banks, T. Shay, M. B. Brenner, L. Lynch, γδ T cells producing interleukin-17A regulate adipose regulatory T cell homeostasis and thermogenesis. *Nat. Immunol.* **19**, 464–474 (2018).
35. M. A. Horisberger, P. Staeheli, O. Haller, Interferon induces a unique protein in mouse cells bearing a gene for resistance to influenza virus. *Proc. Natl. Acad. Sci. U.S.A.* **80**, 1910–1914 (1983).
36. S. Itohara, P. Mombaerts, J. Lafaille, J. Iacomini, A. Nelson, A. R. Clarke, M. L. Hooper, A. Farr, S. Tonegawa, T cell receptor δ gene mutant mice: Independent generation of αβ T cells and programmed rearrangements of γδ TCR genes. *Cell* **72**, 337–348 (1993).
37. S. Andrews, FastQC: A quality control tool for high throughput sequence data (2010); www.bioinformatics.babraham.ac.uk/projects/fastqc.
38. J. M. Mudge, J. Harrow, Creating reference gene annotation for the mouse C57BL6/J genome assembly. *Mamm. Genome* **26**, 366–378 (2015).
39. A. Dobin, C. A. Davis, F. Schlesinger, J. Drenkow, C. Zaleski, S. Jha, P. Batut, M. Chaisson, T. R. Gingeras, STAR: Ultrafast universal RNA-seq aligner. *Bioinformatics* **29**, 15–21 (2013).
40. Picard tools.
41. D. Karolchik, A. S. Hinrichs, T. S. Furey, K. M. Roskin, C. W. Sugnet, D. Haussler, W. J. Kent, The UCSC Table Browser data retrieval tool. *Nucleic Acids Res.* **32**, D493–D496 (2004).
42. M. I. Love, W. Huber, S. Anders, Moderated estimation of fold change and dispersion for RNA-seq data with DESeq2. *Genome Biol.* **15**, 550 (2014).
43. A. Krämer, J. Green, J. Pollard Jr., S. Tugendreich, Causal analysis approaches in ingenuity pathway analysis. *Bioinformatics* **30**, 523–530 (2014).
44. A. A. Sergushichev, An algorithm for fast preranked gene set enrichment analysis using cumulative statistic calculation. bioRxiv 060012 [**Preprint**]. 20 June 2016.
45. A. Liberzon, A. Subramanian, R. Pinchback, H. Thorvaldsdóttir, P. Tamayo, J. P. Mesirov, Molecular signatures database (MSigDB) 3.0. *Bioinformatics* **27**, 1739–1740 (2011).
46. A. Subramanian, P. Tamayo, V. K. Mootha, S. Mukherjee, B. L. Ebert, M. A. Gillette, A. Paulovich, S. L. Pomeroy, T. R. Golub, E. S. Lander, J. P. Mesirov, Gene set enrichment analysis: A knowledge-based approach for interpreting genome-wide expression profiles. *Proc. Natl. Acad. Sci. U.S.A.* **102**, 15545–15550 (2005).

Acknowledgments: We thank the members of the Dixit and Iwasaki labs for critical discussion and feedback related to this project. **Funding:** This work was in part supported by funding from the NIH (AI054359, R01EB000487, R01AI127429, R42AI120269, and R21AI131284 to A.I.). A.I. received support from the Claude D. Pepper Older Americans Independence Center at Yale University School of Medicine P30 AG021342 NIH/NIA. A.I. is an Investigator of the Howard Hughes Medical Institute. The Dixit lab is supported in part by NIH grants P01AG051459, AI105097, AG051459, and AR070811 and the Glenn Foundation on Aging Research. E.L.G. is supported by NIH grant K99AG058801. **Author contributions:** A.I. and V.D.D. conceived the overall project, experiments, and data interpretation. E.L.G. and R.D.M. conceived and performed experiments, data analysis, and interpretation. A.I., V.D.D., E.L.G., and R.D.M. prepared the manuscript. Y.K. and S.S. performed RNA-seq analysis. E.K. performed experiments to measure viral titers and performed other experiments. **Competing interests:** The authors declare that they have no competing interests. **Data and materials availability:** RNA-seq data reported in this study have been deposited in the Gene Expression Omnibus database under the accession number GSE136536. All other data needed to evaluate the conclusions in the paper are present in the paper or the Supplementary Materials.

Submitted 23 August 2018
Resubmitted 26 August 2019
Accepted 1 October 2019
Published 15 November 2019
10.1126/sciimmunol.aav2026

Citation: E. L. Goldberg, R. D. Molony, E. Kudo, S. Sidorov, Y. Kong, V. D. Dixit, A. Iwasaki, Ketogenic diet activates protective γδ T cell responses against influenza virus infection. *Sci. Immunol.* **4**, eaav2026 (2019).

Science Immunology

Ketogenic diet activates protective γδ T cell responses against influenza virus infection

Emily L. Goldberg, Ryan D. Molony, Eriko Kudo, Sviatoslav Sidorov, Yong Kong, Vishwa Deep Dixit and Akiko Iwasaki

Sci. Immunol. **4**, eaav2026.
DOI: 10.1126/sciimmunol.aav2026

Putting mice on a keto diet

Our immune responses to infections are influenced by several extrinsic factors, including weather, social interactions, and diet. Here, Goldberg *et al.* report that feeding mice a high-fat, low-carbohydrate ketogenic diet confers protection in the context of lethal influenza infection. By characterizing the immune response in the lungs, the authors identified that ketogenic diet promoted the expansion of γδ T cells in the lung. Using mice lacking γδ T cells, the authors have established the functional importance of these cells in conferring protection. Their findings suggest that γδ T cells improve barrier function in the lungs by modifying differentiation and function of the airway epithelial cells.

Science Immunology (ISSN 2470-9468) is published by the American Association for the Advancement of Science, 1200 New York Avenue NW, Washington, DC 20005. The title *Science Immunology* is a registered trademark of AAAS.